Open access • Journal Article • DOI:10.1116/1.578205

Frequency effects in silane plasmas for plasma enhanced chemical vapor deposition — Source link

Alan Howling, J.-L. Dorier, Ch. Hollenstein, Ulrich Kroll ...+1 more authors

Institutions: École Polytechnique Fédérale de Lausanne, University of Neuchâtel, Forschungszentrum Jülich

Published on: 01 Jul 1992 - Journal of Vacuum Science and Technology (American Vacuum Society)

Topics: Plasma processing, Plasma-enhanced chemical vapor deposition, Charge coupled device camera, Chemical vapor deposition and Plasma

Published in Journal of Vacuum Science & Technology A 10, issue 4, 1080-1085, 1992
which should be used for any reference to this work

Frequency effects in silane plasmas for plasma enhanced chemical vapor deposition

A. A. Howling, J.-L. Dorier, and Ch. Hollenstein
CRPP/EPFL, 21 Av. des Bains CH-1007 Lausanne, Switzerland

U. Kroll
IMT, 2 Rue Breguet, CH-2000 Neuchatel, Switzerland

F. Finger
Forschungszentrum Jülich, D-5170 Jülich, Germany

It is now generally recognized that the excitation frequency is an important parameter in radio-frequency (rf) plasma-assisted deposition. Very-high-frequency (VHF) silane plasmas (50–100 MHz) have been shown to produce high quality amorphous silicon films up to 20 Å/s [H. Curtins, N. Wyrsch, M. Favre, and A. V. Shah, Plasma Chem. Plasma Processing 7, 267 (1987)], and therefore the aim of this work is to compare the VHF range with the 13.56 MHz industrial frequency in the same reactor. The principal diagnostics used are electrical measurements and a charge coupled device camera for spatially resolved plasma-induced emission with Abel inversion of the plasma image. We present a comparative study of key discharge parameters such as deposition rates, plasma uniformity, ion impact energy, power transfer efficiency, and powder formation for the rf range 13–70 MHz.

I. INTRODUCTION

13.56 MHz is presently the most commonly used frequency for low pressure radio-frequency (rf) plasma processing. This choice is dictated by convention and the consequent availability of rf technology suited to this frequency, rather than by optimization of the physical processes in the discharge. There exists, however, a growing body of experimental and theoretical evidence[1–3] to show that different excitation frequencies can be used to advantage, primarily to obtain good quality films at high deposition rates.

In this paper we describe experiments performed in the frequency range 13.56–70 MHz for a rf capacitative discharge, thereby comparing the industrial frequency with the very-high-frequency (VHF) regime in the same reactor. We direct our investigation to considerations of technological importance with regard to amorphous silicon (*a*-Si:H) deposition, such as deposition rate, uniformity, powder production, and spectroscopy as a process monitor.

A general problem with variable frequency operation is that the rf matching condition, circuit impedances, and consequently the circuit rf power losses are all frequency dependent. Therefore a frequency scan performed at constant source power generally does not guarantee constant plasma power, especially when impedance matching circuits are exchanged in order to cover an extended frequency range. Measurements made at different frequencies cannot, then, be legitimately compared as a straightforward function of frequency. In what follows, we have taken particular care to ensure constant power density in the plasma, as described in Sec. III, thus avoiding device-dependent errors.

Previous work by Curtins *et al.*[1] demonstrated good quality *a*-Si:H deposition rates of 20 Å/s in the range 25–150 MHz, but at constant source power, which could mask the true frequency dependence. Oda[4] compares the industrial frequency 13.56 MHz with a single frequency in the VHF domain (144 MHz) by using two different matching circuits, so plasmas at equal source power cannot be directly compared. Moisan *et al.*[2] covers the whole range from rf to microwave frequencies. This was achieved by launching surface waves in an electrodeless discharge where the substrate remains always at floating potential. The plasma/substrate voltage drop across the sheath is therefore very different from the classical rf capacitative discharge, where it is strongly influenced by rf power and frequency. This sheath voltage determines the ion bombardment energy at the substrate surface, the energy transfer to the electrons, and most probably the powder trapping in a rf capacitor discharge. In the bulk plasma, the ratio of frequency to gas pressure is considered to be an independent parameter via a similarity law,[5] in which case a frequency scan is equivalent to a gas pressure scan. However the influence of frequency in the sheath regions reveals the frequency as an important independent parameter.

Theoretical work has made many advances at MHz frequencies,[5–7] but is not yet capable of predicting the very-high-frequency dependence for polyatomic, electronegative gases in the presence of particulates, such as in silane plasmas: the assessment of new regimes therefore still relies on experiment.

This work is organized as follows: the method for constant plasma power operation is explained after a brief description of the apparatus. Results are then presented for deposition rate, spectroscopic measurements and powder observations. The uniformity of the deposited films is then

compared with Abel-inverted SiH* emission radial profiles in the final section before the conclusions.

II. DESCRIPTION OF THE EXPERIMENT AND PROCEDURE

The rf capacitative reactor consists of two opposing cylindrical steel electrodes of 130 mm diam. The 8×8 cm Corning glass substrate is attached to the underside of the top, grounded electrode which is heated to 230 °C. The lower, rf electrode has a concentric grounded guard screen and is maintained at 15 °C by water cooling. The apparatus is described in more detail in Ref. 8.

The diagnostics employed include a passive electrode voltage probe (mounted on the interior of the rf electrode surface exposed to the plasma), plasma emission spectroscopy, and imaging of the whole plasma with a charge coupled device (CCD) camera—these are described in their relevant sections below.

A series of films was deposited using frequencies from 13.56 to 70 MHz, with deposition times of 1–2 h giving thicknesses between 2 and 5 μm. For this frequency scan, the study was confined to pure silane plasmas with the same set of parameters, chosen to be relevant to deposition conditions, namely: pressure 0.3 mbar, flow rate 30 sccm, electrode spacing 2 cm, substrate temperature 230 °C, and a plasma power of 5 W (see Sec. III). The plasma visible emission completely filled the electrode gap for all the frequencies investigated and so the volume-averaged plasma power density was judged to be constant at 19 mW cm^{-3}.

Using the same reactor for the frequency-dependence study has the important advantage of ensuring identical gas flow dynamics, electric field configuration, and particle diffusion lengths. No attempt was made here to optimize the deposition rate by varying the gas pressure, electrode distance etc.; the aim of this work was to investigate the influence of frequency for a fixed set of discharge parameters.

III. FREQUENCY SCAN AT CONSTANT PLASMA POWER

The source, or input, power is supplied by a dc-decoupled wideband (10 kHz–200 MHz) amplifier via a 50 Ω coaxial cable to the matching network input terminal, at which point the rf power is measured with an in-line, directional meter. At each frequency, the matching network is adjusted for zero reflected power. As explained in the introduction, it is the power losses in the matching network and reactor circuit, and their variation with frequency, which means that the source power is different from the power dissipated in the plasma.

The plasma power could in principle be directly measured using the product of voltage and current monitored at the rf electrode, but in the VHF domain it is difficult, in practice, to calibrate voltage and current probes to obtain the necessary high precision in their relative phase. These problems are compounded when the frequency is variable.

We therefore adopt the subtractive method[9–11] in which the discharge power is determined from the difference in input power with a discharge and the input power without a discharge for the same rf electrode voltage, the latter condition is assured by adjustment of the source power level. Therefore, except for a directional coupler for the source power, the only diagnostic required is a voltage probe which obviates any current/voltage phase calibration. The measurement depends on the fact that the plasma conductance as seen by the voltage probe is in parallel with the equivalent reactor circuit and matching network conductance; the discharge power is thus simply added to the reactor circuit power losses. The voltage probe must be positioned as close as possible to the plasma *ie* on the rear surface of the rf electrode. Another possibilty would be to measure the voltage in a more accessible location such as the output terminal from the matching network; however the electrode voltage must then be extrapolated to the rf electrode by means of an equivalent circuit to account for the impedance of the connections. Once a rf electrode voltage probe is installed, all uncertainties due to any extrapolation calculations are circumvented. It should be recognized that the measurement is nonperturbing in spite of the electrical load due to the probe circuit and its electrically floating oscilloscope because the probe is considered to form an integral part of the total reactor impedance and all measurements are made with the probe *in situ*.

Experimentally, the source power level needed to ensure the required plasma power dissipation P_{pl} for a given frequency was estimated as follows:

First, with the matching network tuned for zero reflected power at the required frequency, a plot was made of the rms electrode voltage squared versus the source power with no plasma. The straight line, as expected for a linear circuit, is given by

$$P_0 = G_0 V_{rms}^2$$

where G_0 is the equivalent matching circuit conductance with respect to ground measured at the voltage probe position, and the source power P_0 represents all the circuit power losses.[11]

Second, the silane plasma was established with the required flow rate and pressure. The source power now represents the total power P_{tot} dissipated in the circuit and plasma

$$P_{tot} = P_0 + P_{pl} = (G_0 + G_{pl}) \cdot V_{rms}^2,$$

where G_{pl} is the plasma conductance.[11] The source power was then adjusted until the difference between P_{tot} and P_0 gave $P_{pl} = 5$ W as required. This defined the operation point of the system at this frequency for which the film was deposited at a plasma power of 5 W.

Two π-matching networks were separately employed in order to cover the range of frequency: a commercial system for 13–30 MHz, and an inhouse network (using two variable, vacuum capacitors and a copper-strip inductance) for 20–100 MHz. The experimentally determined source powers which yielded a plasma power of 5 W are shown in Fig. 1 for each matching network and frequency used for the

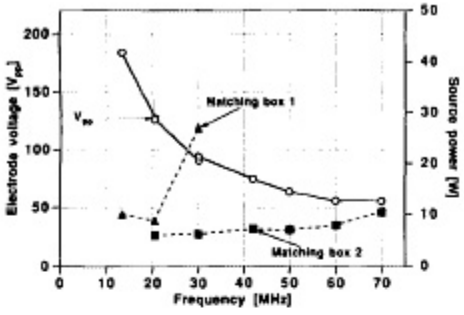

FIG. 1. Source powers and electrode voltages used for both matching networks in order to obtain a plasma power of 5 W at each frequency. The closed symbols represent the source power values. Matching box 1 covers the range 13–30 MHz; the range for matching box 2 is 20–100 MHz.

nine films deposited, along with the peak-to-peak electrode voltage which corresponded to each operation point. It is important to note that the electrode voltage was found to be the same, within experimental error, for a given frequency regardless of which matching network was used—see $f = 20.5$ and 30 MHz for which the matching network frequency ranges overlap. This is a check of the method used to set the plasma power, because, when all the plasma parameters are the same, the power in the plasma uniquely determines the plasma conductance and the electrode voltage. Furthermore, for 20.5 and 30 MHz, the same visible spectrum intensities and the same deposition rate (see Sec. IV) were observed, even though the source power, in order to achieve the same plasma power, differs by up to a factor 4 between the two matching networks.

Therefore, we can note the following.

(a) Operation at constant source power with different matching circuits, and/or different frequencies, would give erroneous results because the plasma power would not be constant.

(b) Once the plasma power and the other external parameters are correctly determined, the plasma properties are independent of the matching network and reactor circuit losses. This means that the results are applicable to all rf capacitative reactors of similar geometry.

Electrode voltage and ion impact energy: All rf capacitative discharges can be considered in the simplest approximation as a resistive bulk plasma bounded by capacitative sheaths. Therefore, for constant plasma power, the voltage drop across the sheaths diminishes at higher frequency as shown in Fig. 1. This is a property of the plasma independently of the rest of the circuit. Therefore, for a given plasma power, the electrode voltage can be chosen by adjusting the discharge excitation frequency. There is, however, a lower voltage limit below which the plasma cannot be maintained for a given plasma power: for our case of $P_{pl} = 5$ W, a silane plasma could not be sustained for frequencies of 80 MHz or higher and this defined the upper frequency limit for these experiments—a higher plasma power would have allowed higher frequency operation.

The ion impact energy on the growing film surface depends on the sheath potential and the rf electrode self-bias. The self-bias V_{sb} is small compared with the peak-to-peak electrode voltage V_{pp} in our reactor ($|V_{sb}/V_{pp}| < 5\%$) for the range of frequencies investigated, as expected for the symmetric electrode configuration. Therefore the time-averaged plasma potential, in the capacitative sheath approximation appropriate to the high frequencies used in these experiments, is $V_{pp}/4$.[12] In our case of a substrate on the grounded electrode, this is the average substrate/plasma sheath potential. Since the excitation frequency is estimated to be higher than the ion transit frequency, the ions experience the sheath potential averaged over many rf cycles as they drift towards the electrode in the sheath electric field. This results in a maximum ion energy at the substrate surface, of energy $eV_{pp}/4$. From Fig. 1, it can be seen that low frequencies therefore result in a much higher ion impact energy on the substrate, which could create defects during deposition.[13] On the other hand, a sufficient amount of low energy ion bombardment is considered to be beneficial for the growth by e.g., increasing the surface mobility of reactive species. Attempting to increase the growth rate at 13.56 MHz by raising the rf power would simply increase V_{pp} and the ion impact energy, thus aggravating the situation. At 70 MHz, however, the effective power and growth rate could be increased whilst keeping the ion impact energy within reasonable limits concomitant with deposition of good quality material.

IV. RESULTS

A. Deposition rate

The mean film thickness was estimated from several measurements using a surface profiler across the surface of each amorphous silicon film to account for any deposition nonuniformity (see Sec. V). Figure 2(a) shows the mean deposition rate so obtained by dividing by the corresponding discharge time. This deposition rate, for a constant plasma power of 5 W, increases by a factor 3 from 3.3 to 10 Å/s as the frequency is increased from 13.56 to 70 MHz.

The film optical quality was comparable for the whole frequency range as measured by photothermal deflection spectroscopy, with defect densities of $1–2 \cdot 10^{16}$ cm^{-3} and Urbach energy of less than 60 meV. All films also exhibited good adhesion, with seemingly no internal stress problems.

The film quality for a deposition rate of 10 Å/s at 70 MHz thus compares well with the 3.3 Å/s films at 13.56 MHz for the same plasma power. If the power at 13.56 MHz were high enough to obtain 10 Å/s, it is often observed that inferior films result. The combination of good quality and high deposition rate for films deposited at 70 MHz may be in part due to the lower sheath potentials as compared to 13.56 MHz. Moisan *et al.*[2] also report an improvement in deposition rates of a similar magnitude for the VHF regime, although the plasma and reactor are of a very different type.

From this data alone it is not possible to attribute the deposition rate increase to, for example, higher dissociation rates in the plasma, or to improved surface chemistry con-

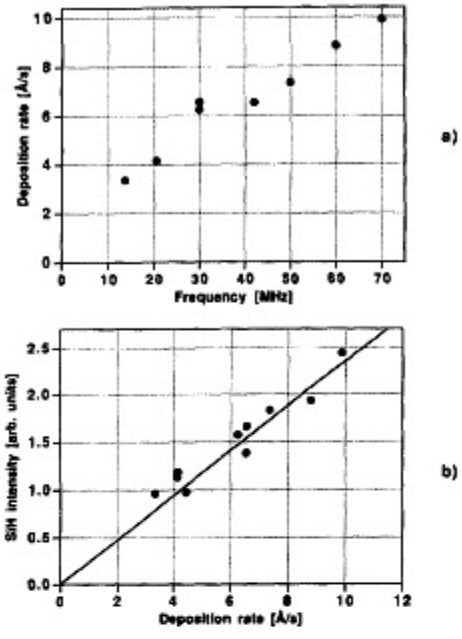

FIG. 2. (a) Deposition rate vs rf frequency for a plasma power of 5 W; (b) Correspondance of the global SiH* intensity with deposition rate for the same conditions.

ditions at the film/sheath interface. For more information, we now consider the plasma-induced emission as a function of frequency.

B. Plasma emission spectroscopy

The global plasma emission was collected with fiber optics and monitored by a spectrometer and optical multichannel analyzer. Placing the observation port at the end of a 22-cm-long tube eliminated any deposition on the window which would otherwise have falsified comparison between the spectra.

The emission intensities from the excited radicals Si* [288 nm], SiH* [band at 414 nm], H_2^* [Fulcher-α line at 612 nm] and H* [Hα at 656 nm] were recorded during the deposition for each frequency. The SiH* and Fulcher-α intensities increased by factors 2.5 and 3.8, respectively, over the frequency range 13.56–70 MHz, whereas the Si* and Hα emission increased by 30% to 60% only. All of these intensities therefore increased with frequency at constant plasma power, although by different degrees, reflecting the different channels by which the radicals are created and excited.

Figure 2(b) shows that the dominant plasma emission due to SiH* correlates well with the deposition rate as the frequency is varied at constant plasma power. Several authors[4,14] have reported this correlation as a function of rf power or silane flow rate. The SiH radical is not responsible for deposition,[15] but this correlation suggests that SiH* formation is related to the dissociation channel for the radical species which form the film. Further evidence, exploiting the spatial nonuniformity of the film and the SiH* emission, follows in Sec. VI.

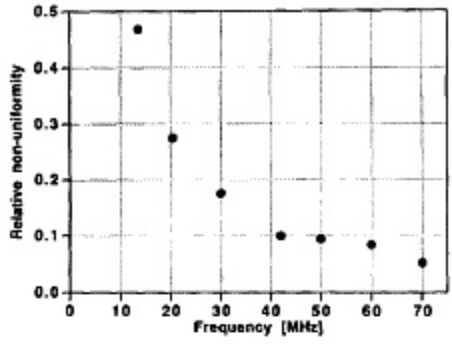

FIG. 3. Difference between edge and central film thicknesses normalized to the average thickness for each film, plotted as a function of frequency. The films deposited at high frequency are the most uniform.

C. Powder production

Powder produced and suspended in the silane plasma was observed under white light illumination[16] and recorded with a CCD camera. For a plasma power of 5 W, with the grounded electrode carrying the substrate heated to 230 °C and the rf electrode maintained at 15 °C, the powder was always confined to a layer suspended at the plasma/sheath interface above the cold rf electrode. No powder particles were found on the hot electrode and substrate surface, and good quality films have been produced under these conditions. During the film deposition with a 70 MHz discharge, only a thin disc of powder at the plasma/sheath boundary was visible, but the trend for lower frequencies was for the powder layer to grow in width and intensity.[9] It would seem plausible that the larger sheath potentials trap and confine powder more efficiently at the lower frequencies. To what extent the diminution of powder at high frequencies is a phenomenon concurrent with, or a cause of, the increase in deposition rate and plasma emission is difficult to ascertain from this work.

V. RADIAL DISTRIBUTION OF PLASMA EMISSION AND DEPOSITED FILM

The film thickness must be uniform ($\pm 5\%$) in order to avoid current mismatch in devices such as photovoltaic cells. We have therefore investigated the deposition homogeneity across the surface of the substrate as a function of frequency. The film is thicker at larger radii, and Fig. 3 shows the difference between edge and central thicknesses normalized to the surface-averaged value for each frequency. This relative depth is much smaller at higher fre-

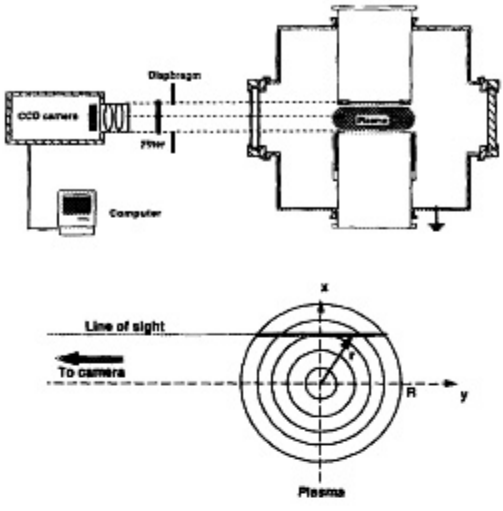

FIG. 4. Schematic of the experimental arrangement, showing the geometry for the Abel inversion of the plasma emission.

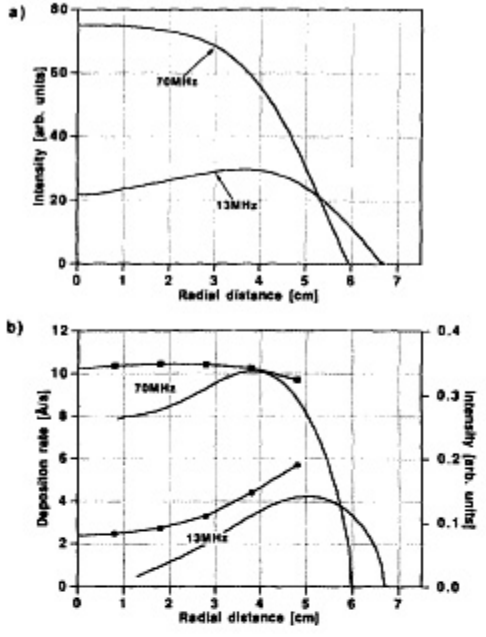

FIG. 5. Comparison of: (a) the line-of-sight lateral emission intensity profiles with (b) the Abel-inverted radial intensity profiles, for frequencies 13 and 70 MHz. The measured film thickness radial profiles for both frequencies are superposed on (b) to demonstrate the correspondance between the radial deposition rates and the radial SiH* emission intensities.

quencies and implies a more spatially homogeneous deposition rate over the substrate surface than for lower frequencies.

For a more specific test of the observation, made in Sec. IV B, that the global SiH* (414 nm) emission intensity correlates well with the surface-averaged deposition rate, we compared the radial intensity variation of the SiH* emission with the radial deposition rate inferred from the film thickness:

The two-dimensional plasma emission image, which is dominated by the SiH* radiation, was monitored and digitised by means of a CCD camera giving a spatial resolution of better than 2 pixels/mm along the whole plasma diameter—see Fig. 4 for a schematic of the experimental arrangement. An interference filter could be used to study specific wavelengths. The lateral intensity profiles across each horizontal plane were symmetric about the origin defined by the electrode axis, as expected for an axisymmetric discharge. The line-of-sight intensity is averaged along the y axis, and for an optically thin cylindrically symmetric extended source, the lateral profile $I(x)$ is related to the radial intensity distribution $\epsilon(r)$ through the Abel inversion[17]

$$\epsilon(r) = -1/\pi \int_r^R \frac{dI(x)}{dx} \frac{dx}{\sqrt{x^2 - r^2}}.$$

Numerical calculation procedures strongly amplify any noise in the raw data and so it is convenient to fit an analytical function. The lateral intensity profiles taken from a plane near to the plasma/sheath boundary in front of the substrate are shown for 13.56 and 70 MHz plasmas in Fig. 5(a), with the corresponding Abel-inverted profiles in Fig. 5(b). The intensity near the origin is not shown because of the large inaccuracy there; physically, this is because the emitting volume near the axis has a vanishingly small contribution to line-averaged profiles.

Note that line-of-sight averaging means that even a uniform plasma emission corresponds to a "hollow" radial intensity distribution. Equally, it should be borne in mind that vertical intensity profiles measured from the exterior do not necessarily represent the true vertical emission profiles in the plasma interior.

The radial deposition rate was estimated from the thickness measured across the substrate diagonal, and Fig. 5(b) compares this with the radial SiH* intensity for 13.56 and 70 MHz. This shows that the SiH* emission is useful not only as a global process monitor for deposition rate, but also as a local indicator of the spatial variation in deposition rate. Radial intensity profiles of SiH* were first obtained by Asano *et al.*[18] for 13.56 MHz plasmas, but without comparison to the local deposition rates. Accounting for this nonuniformity, the on-axis deposition rate is a factor 4 times higher at 70 MHz than at 13.56 MHz.

Contrary to these findings, it might be expected that VHF plasmas would exacerbate the uniformity problem because of the shorter vacuum wavelength which could result in nodes of high potential in large devices. Also, any

spurious self-inductance in the electrodes or their rf connections would incur proportionately larger phase errors at VHF.[19] Nevertheless, with our reactor geometry, we find better uniformity in the VHF domain, and it remains to be seen if this holds true for larger reactors.

VI. CONCLUSIONS

The properties of silane plasmas have been compared for the frequency range 13.56–70 MHz in the same rf capacitative reactor.

For the same power in the plasma, the deposition rate is three times higher at 70 MHz than at 13.56 MHz, with comparable film optical qualities.

Powder formation is also strongly reduced at high frequencies. The lower sheath voltage in the VHF domain also means that the plasma power, and hence the deposition rate, can be still further increased before energetic ion bombardment begins to alter the film surface.

Abel inversion of the SiH* plasma emission, to give the radial intensity distribution, correlates well with the radial variation in film thickness, showing that SiH* emission is a spatial indicator of the local deposition rate. These experiments demonstrate a much-improved film uniformity at high frequency.

In summary, VHF plasma deposition exhibits several important advantages compared to 13.56 MHz for our reactor geometry. However, for the present, operation at frequencies different from the authorized frequencies such as 13.56 MHz involves supplementary technological effort and expense. Before exploitation, plasma processing at very-high-frequency must first be proven in a larger-scale reactor.

ACKNOWLEDGMENTS

We wish to thank R. Tscharner for his advice on rf matching networks. This work benefited from the assistance of G. Feusier and was funded by Swiss Federal Research Grant Nos. EF-REN(89)17 and EF-REN(91)031.

[1]H. Curtins, N. Wyrsch, M. Favre, and A. V. Shah, Plasma Chem. Plasma Processing **7**, 267 (1987).
[2]M. Moisan, C. Barbeau, R. Claude, C. M. Ferreira, J. Margot, J. Paraszczak, A. B. Sa, G. Sauvé, and M. R. Wertheimer, J. Vac. Sci. Technol. B **9**, 8 (1991).
[3]D. L. Flamm, J. Vac. Sci. Technol. A **4**, 729 (1986).
[4]S. Oda, J. Noda, and M. Matsumura, Jpn. J. Appl. Phys. **29**, 1889 (1990); Mater. Res. Soc. Symp. Proc. **118**, 117 (1988).
[5]C. M. Ferreira and M. Moisan, Phys. Scri. **38**, 382 (1988).
[6]M. Capitelli, C. Gorse, R. Winkler, and J. Wilhelm, Plasma Chem. Plasma Processing **8**, 399 (1988).
[7]J.-P. Boeuf, Phys. Rev. A **36**, 2782 (1987).
[8]J.-L. Dorier, Ch. Hollenstein, A. A. Howling, and U. Kroll, J. Vac. Sci. Technol. A **10**, 1048 (1992).
[9]J. S. Logan, in *Handbook of Plasma Processing Technology*, edited by S. M. Rossnagel, J. J. Cuomo and W. D Westwood, (Noyes, Park Ridge, NJ, 1990), p. 155.
[10]C. M. Horwitz, J. Vac Sci. Technol. A **1**, 1795 (1983).
[11]V. A. Godyak and R. B. Piejak, J. Vac. Sci. Technol. A **8**, 3833 (1990).
[12]K. Köhler, D. E. Horne, and J. W. Coburn, J. Appl. Phys. **58**, 3350 (1985).
[13]A. Gallagher, Int. J. Solar Energy **5**, 311 (1988).
[14]C. L. Yang, Y. H. Shing, and C. E. Allevato, 20th IEEE Photovoltaic Specialists Conference, Sept. 26–30 Las Vegas, 1988 (unpublished), p. 202.
[15]J. P. M. Schmitt, P. Gressier, M. Krishnan, G. De Rosny, and J. Perrin, Chem. Phys. **84**, 281 (1984).
[16]A. A. Howling, Ch. Hollenstein, and P.-J. Paris, Appl. Phys. Lett. **59**, 1409 (1991).
[17]W. Lochte-Holtgreven, in *Plasma Diagnostics*, edited by W. Lochte-Holtgreven, (North-Holland, Amsterdam, 1968), p. 184.
[18]Y. Asano, D. S. Baer, R. Hernberg, and R. K. Hanson, Plasma Chem. Plasma Processing **8**, 1 (1988).
[19]J. P. M. Schmitt, Material Research Society Symposium Proceedings, Anaheim, 1991 (in press).